XL CILAMCE
IBERO-LATIN AMERICAN CONGRESS ON COMPUTATIONAL METHODS IN ENGINEERING
NOVEMBER 11-14, 2019
Praiamar Natal Hotel & Convention Natal, RN-BRAZIL

Finite Element Method applied to the single-layer equivalent theory for laminated beams

Santana H. M
Da Rocha F. C
hiltonmarquess@gmail.com
fcrocha@ufs.br
Federal University of sergipe
Av. Marechal randon s/n, 49400-00, São Cristovão/Sergipe, Brazil
Kzam A. K. L.
Aref.kzam@unila.edu.br
Federal University of Latin American Integration
Av. Silvio Américo Sasdelli 1842, 85866-000, Foz do Iguaçu/Paraná, Brazil

Abstract. Over the last decades, laminated beams have been widely used as a structural element in several areas of knowledge, such as in civil, naval, mechanical and aeronautical engineering. Having advanced the knowledge and development of composite materials, theoretical modeling to describe the mechanical behavior of laminated beams has become of great importance. Among the various theories, we have the refined (or high order) theories that have emerged to heal the limitations present in classical theories. This limitation is represented by the failure to consider the shear strain field or by incorrect consideration of such deformations, without respecting the nullity of the shear stress at the edges of the beam. Thus, the present work seeks to present the development of a finite element model applied to the Equivalent Layer (ESL) theories for laminated beams. Therefore, a unified displacement field will be used that allows the simultaneous development and comparison of several refined theories found in the literature. After obtaining the governing equations, the finite element model is constructed using the Hermite and Lagrange polynomial functions. Finally, to show the good efficiency of the theories and the finite element model, numerical results for static and dynamics analysis are shown and compared with the exact solution of the elasticity.

Keywords: Laminated beams, ESL theories, Finite Element Method

1 Introduction

Because recent advancement of technology, composite beams have gained wide applicability in civil, aeronautical, marine and mechanical engineering due to the better mechanical properties of these materials such as strength, stiffness, weight and thermal conductivity. However, when beams subjected to transverse loads the shear strain become larger due to the smaller transverse shear modulus than tensile modulus in the plane. Two types of composite beams theories are commonly found in the literature: theories from displacement field and theories from both the displacement and stress fields.

Among the theories derived from displacement field are the classical Euler-Bernoulli Theory (EBT), the First Order or Timoshenko Theory (FOT) and the High Order Theory (HOT). Initially these theories were developed for isotropic and single layer beams, however, through the Equivalent Single Layer Theories (ESL) it is possible to extend to orthotropic and laminated beams. The EBT developed in the eighteenth century is considered the simplest model, because it does not consider the shear deformation in displacement field. Another simplification is to consider that the cross section of the beam remains flat and orthogonal to the neutral line that is considered only for slender beams. At the beginning of the twentieth century, Timoshenko [1] developed FOT and began to consider a constant deformation due to shear, so his theory does not allow the nullity of shear stress at the beam edges, causing the need to use correction factors for a better efficiency of your results. From the middle of the twentieth century, the High Order Theories emerged with the main objective of remedying the limitation found in the FOT, that is, the need for correction factors. For this, these models seek to describe the beam displacement field through polynomial, trigonometric, exponential and hyperbolic functions [2-9] and thus guarantee the nullity of shear stress at the beam edges. Sayyad and Ghugal [10] make a comparison of several high order theories found in the literature and demonstrate that they have a similar performance, and there is no theory that disagrees with the others.

It is also important to note that Equivalent Single Layer Theories have an accurate efficiency only in describing the overall behavior of the beam, i.e transverse displacement, free vibration and buckling (Reddy [11]). This is due to the adoption of a Class C^1 displacement field that results in a continuous deformation field and since the layers have different transverse shear modulus, the shear stress field will be discontinued. One way to solve this drawback is to obtain the shear stress field from the elasticity equilibrium equations (Reddy [11]).

In the present work, several high order theories models will be developed simultaneously in order to study their static and dynamic behavior of symmetrical laminated beams subjected to a transverse loading. The equations that describe the problem are derived from the Hamilton principle. A class C^1 finite element model using interdependent interpolation is also developed. The numerical results obtained are compared with the elasticity theory obtained in Pagano [12] and Giunta et al. [13]

2 Governing Equations

4.2 Kinematics

Consider a full-thickness beam equal to h composed of N orthotropic layers with the main material coordinates (x_1^k, x_x^k, x_3^k) of the kth layer oriented at an angle θ_k relative to the coordinate *x*. The layer kth is located between the points $z = z_k$ and $z = z_{k+1}$ in the direction of thickness (Fig. 1).

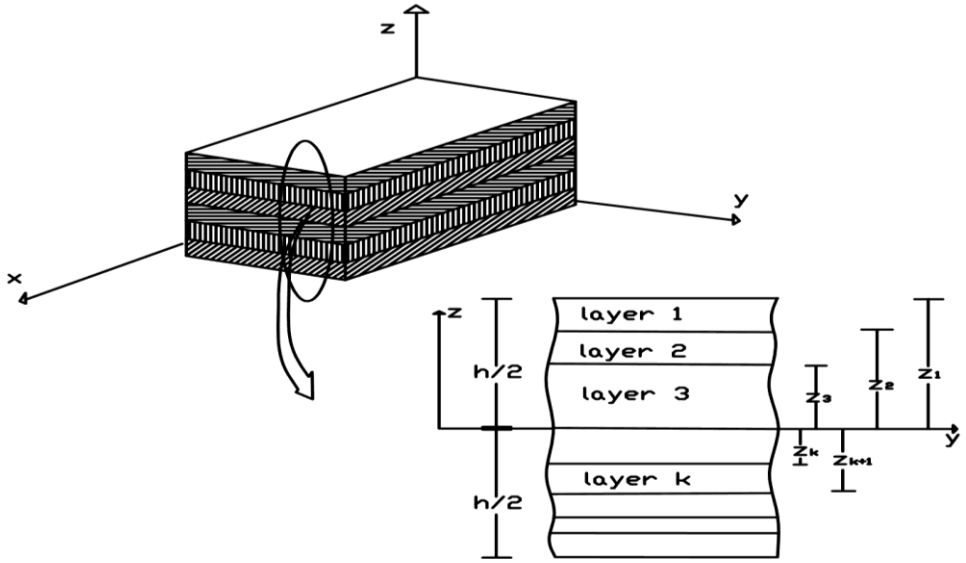

Figure 1. Geometry of a laminated composite beam

In order to cover the kinematics of various refined theories, the unified field of displacement given in Eq. 1:

$$\begin{cases} u(x,z,t) = -z\dfrac{\partial w}{\partial x} + f(z)\phi \\ w(x,z,t) = w(x,t) \end{cases}. \tag{1}$$

where, $u(x,z,t), w(x,t)$ and $\phi(x,t)$ represent, respectively, axial displacement, centroidal axis transverse displacement and cross-sectional rotation due to shear. $f(z)$ is a function that describes the used shear theory presented in Table 1.

Table 1. Shear theory present in the displacement field.

Model	Author	Function $f(z)$
Model 1	Reddy [2]	$f(z)=\left[\frac{z}{2}\left(\frac{h^2}{4}-\frac{z^2}{3}\right)\right]$
Model 2	Shi -Voyiadjis[3]	$f(z)=\left[\frac{5z}{4}\left(1-\frac{4z^2}{3h^2}\right)\right]$
Model 3	Ambartsumyan [4]	$f(z)=z\left[1-\frac{4z^2}{3h^2}\right]$
Model 4	Touratier [5]	$f(z)=\frac{h}{\pi}\sin\left[\frac{\pi z}{h}\right]$
Model 5	Soldatos [6]	$f(z)=\left[z\cosh\left(\frac{1}{2}\right)-h\sinh\left(\frac{z}{h}\right)\right]$
Model 6	Karama et al. [7]	$f(z)=z\exp\left[-2\left(\frac{z}{h}\right)^2\right]$

Model 7	Akavci [8]	$f(z)=\frac{3\pi}{2}\left[h\tanh\left(\frac{z}{h}\right)+ -z\sec^2\left(\frac{1}{2}\right)\right]$
Model 8	Ferreira et al. [9]	$f(z)=h\tan^{-1}\left(\frac{2z}{h}\right)-z$

The deformation field is shown in the Eqs. 2(a and b) follows.

$$\varepsilon_{xx}=\frac{\partial u}{\partial x}=-z\frac{\partial^2 w}{\partial x^2}+f(z)\frac{\partial \phi}{\partial x}. \tag{2a}$$

$$\gamma_{xz}=\left(\frac{\partial w}{\partial x}+\frac{\partial u}{\partial z}\right)=\frac{df(z)}{dz}\ \ \phi\ \ . \tag{2b}$$

Using constitutive laws for orthotropic materials Reddy[11] the stress field shown can be obtained by Eqs. 3(a and b).

$$\sigma_{xx}=Q_{11}\varepsilon_{xx}. \tag{3a}$$

$$\tau_{xz}=Q_{55}\gamma_{xz}. \tag{3b}$$

where:

$$Q_{11}=\frac{1}{(-1+v_{xy}v_{yx})}\begin{pmatrix}E_{xx}cos(\theta)^4+(E_{yy}v_{xy}+E_{xx}v_{yx})cos(\theta)^2sin(\theta)^2+E_{yy}sin[\theta]^4+\\ G_{xy}(1-v_{xy}v_{yx})sin[2\theta]^2\end{pmatrix}. \tag{4}$$

$$Q_{55}=G_{zx}\cos(\theta)^2+G_{yz}\sin(\theta)^2. \tag{5}$$

Where $E_{ii,}$ and G_{ij} *(i=x,y)* are the Modules of longitudinal and transverse elasticity, respectively, in relation to the main axes; θ is the angle that the fiber makes with the main beam axis

The Hamilton's principle Reddy [14] is used to obtain the equations of motion for the displacement field given in Eq. (1). Thus, the equations that describe the theory are presented in Eq. (6 a and b):

$$A_0\frac{\partial^4 w}{\partial x^4}-B_0\frac{\partial^3 \phi}{\partial x^3}-\left(\rho\frac{A_0}{Q_{11}}\frac{\partial^4 w}{\partial x^2\partial t^2}\right)+\left(\rho\frac{B_0}{Q_{11}}\frac{\partial^3 \phi}{\partial t^2\partial x}\right)+\left(\rho bh\frac{\partial^2 w}{\partial t^2}\right)=q\,. \tag{6a}$$

$$B_0\frac{\partial^3 w}{\partial x^3}-C_0\frac{\partial^2 \phi}{\partial x^2}+D_0\phi-\rho\left(\frac{B_0}{Q_{11}}\frac{\partial^3 w}{\partial x\partial t^2}-\frac{C_0}{Q_{11}}\frac{\partial^2 \phi}{\partial t^2}\right)=0\,. \tag{6b}$$

Where:

$$A_0=\int_A z^2Q_{11}^k dA\ =b\sum_{k=1}^{N}\int_{z_{k+1}}^{z} z^2Q_{11}^k dz\,. \tag{7a}$$

$$B_0=\int_A zf(z)Q_{11}^k dA\ =b\sum_{k=1}^{N}\int_{z_{k+1}}^{z} zf(z)Q_{11}^k dz\,. \tag{7b}$$

$$C_0 = \int_A f(z)^2 Q_{11}^k dA = b\sum_{k=1}^{N} \int_{z_{k+1}}^{z} f(z)^2 Q_{11}^k dz \,. \tag{7c}$$

$$D_0 = \int_A f'(z)^2 Q_{55}^k dA = b\sum_{k=1}^{N} \int_{z_{k+1}}^{z} f'(z)^2 Q_{55}^k dz \,. \tag{7d}$$

Where *b,h,N,* ρ and ,*q* represent, respectively, the width of the section, its height, the amount of layers present in the laminated beam, its density and the active distributed loading. In addition to the above domain equations, we have the following boundary conditions:

$$\left\{ \begin{matrix} w \\ \dfrac{\partial w}{\partial x} \\ \phi \end{matrix} \right\} \quad \text{or} \quad \left\{ \begin{matrix} \hat{V}_x = \left[-A_0 \dfrac{\partial^3 w}{\partial x^3} + B_0 \dfrac{\partial^2 \phi}{\partial x^2} - \dfrac{\rho A_0}{Q_{11}} \dfrac{\partial^3 w}{\partial x \partial t^2} + \dfrac{\rho B_0}{Q_{11}} \dfrac{\partial^2 \phi}{\partial x^2} \right] \\ M_{xy} = \left[-A_0 \dfrac{\partial^2 w}{\partial x^2} + B_0 \dfrac{\partial \phi}{\partial x} \right] \\ \hat{M}_{xy} = \left[-B_0 \dfrac{\partial^2 w^{ESL}}{\partial x^2} + C_0 \dfrac{\partial \phi}{\partial x} \right] \end{matrix} \right\}. \tag{8}$$

For dynamic purposes the Eqs. (6a and 6b) can be formulated as an eigenvalue problem in order to find the natural frequencies. So the Eqs (9a and 9b) represent periodic movement of the beam under free vibration (Reddy[14]):

$$w(x,t) = W(x)e^{-i\omega t} \,. \tag{9a}$$

$$\phi(x,t) = S(x)e^{-i\omega t} \,. \tag{9b}$$

Where ω is the natural frequency of transverse motion, $W\ x$ and $S\ x$ they are the shapes of the mode of transverse motion. Replacing the Eqs (9a and 9b) in Eqs. (6a and 6b) (with $q = 0$) :

$$\left[A_0 \frac{d^4 W}{dx^4} - B_0 \frac{d^3 S}{dx^3} + \left(\omega^2 \rho \frac{A_0}{Q_{11}} \frac{d^2 W}{dx^2} \right) - \left(\omega^2 \rho \frac{B_0}{Q_{11}} \frac{dS}{dx} \right) - \omega^2 \rho A W \right] = 0 \tag{10a}$$

$$\left[B_0 \frac{d^3 W}{dx^3} - C_0 \frac{d^2 S}{dx^2} + D_0 S + \rho \left(\omega^2 \frac{B_0}{Q_{11}} \frac{\partial W}{\partial x} - \omega^2 \frac{C_0}{Q_{11}} S \right) = 0 \right] \tag{10b}$$

2.2 Shear stress

Due to the adoption of a class C1 displacement field for ESL theories, the shear deformation expressed in eq. 2b will also be a continuous function. Thus, due to the difference between the transverse elasticity modulus of each layer, there will be no continuity in shear stress which will cause possible modeling deficiency in the interlaminary region. Thus, Reddy [11] proposed an alternative way to obtain interlinear stresses through equilibrium equations of three-dimensional elasticity (Eqs. 11).

$$\begin{aligned} 0 &= \frac{\partial \sigma_{xx}}{\partial x} + \frac{\partial \tau_{xy}}{\partial y} + \frac{\partial \tau_{xz}}{\partial z} \\ 0 &= \frac{\partial \tau_{xy}}{\partial x} + \frac{\partial \sigma_{yy}}{\partial y} + \frac{\partial \tau_{xz}}{\partial z} \,. \\ 0 &= \frac{\partial \tau_{xz}}{\partial x} + \frac{\partial \tau_{yz}}{\partial y} + \frac{\partial \sigma_{zz}}{\partial z} \end{aligned} \tag{11}$$

For each layer Eqs. 11 can be integrated with respect to z and interlinear stresses within each layer can be obtained. ($z_k \leq z \leq z_{k+1}$). The shear stress τ_{xz} will be given in Eq. 12.

$$\tau_{xz} = -\int_{z_k}^{z} \left(\frac{\partial \sigma_{xx}}{\partial x} + \frac{\partial \sigma_{xy}}{\partial y} \right) dz + G^{(k)}. \tag{12}$$

Where $G^{(k)}$ It is an integration constant that can be obtained through the nullity of shear stress at the beam edges and the interlaminar continuity condition.

3 Finite element model

This section discusses the development of the finite element method applied to the equivalent layer theory (ESL) for laminated beams. In this work we use the Hermite cubic approximation for the deflection and its derivative and Lagrange quadratic for the variable $\phi(x,t)$, to avoid the shear locking effect(Reddy [15])..

3.1 Weak Formulation

Building the weak formulation for a domain element begins $\Omega^e = (x_a, x_b)$, by multiplying the Eqs. (6a and 6b) by arbitrary functions $\upsilon(x,t)$ and $\psi(x,t)$ called weights, to obtain the following equations:

$$\int_{x_a}^{x_b} \upsilon \left[A_0 \frac{\partial^4 w}{\partial x^4} - B_0 \frac{\partial^3 \phi}{\partial x^3} - \left(\rho \frac{A_0}{Q_{11}} \frac{\partial^4 w}{\partial x^2 \partial t^2} \right) + \left(\rho \frac{B_0}{Q_{11}} \frac{\partial \phi}{\partial x \partial t^2} \right) + \left(\rho bh \frac{\partial w}{\partial t^2} \right) - q \right] dx = 0 \quad . \tag{13a}$$

$$\int_{x_a}^{x_b} \psi \left[B_0 \frac{\partial^3 w}{\partial x^3} - C_0 \frac{\partial^2 \phi}{\partial x^2} + D_0 \phi + \rho \left(-\frac{B_0}{Q_{11}} \frac{\partial^3 w}{\partial x \partial^2 t} + \frac{C_0}{Q_{11}} \frac{\partial^2 \phi}{\partial^2 t} \right) = 0 \right] dx = 0 \quad . \tag{13b}$$

Integrating by parts the Eq.(13a) and Eq.(13b), than:

$$\begin{aligned} &\int_{x_a}^{x_b} \left(A_0 \frac{\partial^2 w}{\partial x^2} \frac{\partial^2 \upsilon}{\partial x^2} - B_0 \frac{\partial \phi}{\partial x} \frac{\partial^2 \upsilon}{\partial x^2} + \rho \left(\frac{A_0}{Q_{11}} \frac{\partial \upsilon}{\partial x} \frac{\partial^3 w}{\partial x \partial t^2} + bh\upsilon \frac{\partial^2 w}{\partial t^2} - \frac{B_0}{Q_{11}} \frac{\partial \upsilon}{\partial x} \frac{\partial^2 \phi}{\partial t^2} \right) \right) dx = \\ &= \int_{x_a}^{x_b} \upsilon q + \upsilon \hat{V} \Big|_{x_a}^{x_b} - \frac{\partial \upsilon}{\partial x} M_{xy} \Big|_{x_a}^{x_b} \end{aligned} \quad . \tag{14}$$

$$\int_{x_a}^{x_b} \left(-B_0 \frac{d^2 w}{dx^2} \frac{d\psi}{dx} + C_0 \frac{d\phi}{dx} \frac{d\psi}{dx} + D_0 \psi \phi + \rho \left(-\frac{B_0}{Q_{11}} \frac{\partial^3 w}{\partial x \partial t^2} \psi + \frac{C_0}{Q_{11}} \frac{\partial^2 \phi}{\partial t^2} \psi \right) \right) dx = \psi \hat{M}_{xy} \Big|_{x_a}^{x_b} \quad . \tag{15}$$

3.2 FEM formulation for the theory

For the development of the MEF in conjunction with the ESL theory, the approximations for $w(x,t)$ e $\phi(x,t)$ this way:

$$w(x,t) \approx \sum_{i=1}^{m} d_i(t)\varphi_i^{(1)}(x), \quad \phi(x,t) \approx \sum_{j=1}^{n} p_j(t)\varphi_j^{(2)}(x)\,. \tag{16}$$

where $\varphi_j^{(1)}$ and $\varphi_j^{(2)}$ are Hermite cubic and Lagrange quadratic polynomial interpolation functions, respectively, d_j are the nodal values consisting of $w(x,t)$ and p_j are the nodal values consisting of $\phi(x,t)$. By the Galerkin Method, one makes $\upsilon \approx \varphi^{1}$ e $\psi \approx \varphi_i^{(2)}$ in the weak formulation of Eqs 14 and 15 to obtain:

$$\begin{bmatrix} [K^{11}] & [K^{12}] \\ [K^{21}] & [K^{22}] \end{bmatrix} \begin{Bmatrix} \{d\} \\ \{p\} \end{Bmatrix} + \begin{bmatrix} [M^{11}] & [M^{12}] \\ [M^{21}] & [M^{22}] \end{bmatrix} \begin{Bmatrix} \{\ddot{d}\} \\ \{\ddot{p}\} \end{Bmatrix} = \begin{Bmatrix} \{F^1\} \\ \{F^2\} \end{Bmatrix}. \tag{17}$$

where:

$$\begin{aligned} K_{ii}^{11} &= \int_{x_a}^{x_b} \left(A_0 \frac{d^2\varphi_i^{(1)}}{dx^2} \frac{d^2\varphi_i^{(1)}}{dx^2} \right) dx, & K_{ij}^{12} &= \int_{x_a}^{x_b} \left(-B_0 \frac{d^2\varphi_i^{(1)}}{dx^2} \frac{d\varphi_j^{(2)}}{dx} \right) dx \\ K_{ji}^{21} &= \int_{x_a}^{x_b} \left(-B_0 \frac{d\varphi_j^{(2)}}{dx} \frac{d^2\varphi_i^{(1)}}{dx^2} \right) dx, & K_{jj}^{22} &= \int_{x_a}^{x_b} \left(C_0 \frac{d\varphi_j^{(2)}}{dx} \frac{d\varphi_j^{(2)}}{dx} + D_0 \varphi_j^{(2)} \varphi_j^{(2)} \right) dx \end{aligned} \tag{18}$$

$$\begin{aligned} M_{ii}^{11} &= \int_{x_a}^{x_b} \rho \left(\frac{A_0}{Q_{11}} \frac{d\varphi_i^{(1)}}{dx} \frac{d\varphi_i^{(1)}}{dx} + bh\varphi_i^{(1)} \varphi_i^{(1)} \right) dx, & M_{ij}^{12} &= \int_{x_a}^{x_b} \left(-\rho \frac{B_0}{Q_{11}} \frac{d\varphi_i^{(1)}}{dx} \varphi_j^{(2)} \right) dx \\ M_{ji}^{21} &= \int_{x_a}^{x_b} \left(-\rho \frac{B_0}{Q_{11}} \frac{d\varphi_j^{(2)}}{dx} \varphi_i^{(1)} \right) dx, & M_{jj}^{22} &= \int_{x_a}^{x_b} \left(\rho \frac{C_0}{Q_{11}} \varphi_j^{(2)} \varphi_j^{(2)} \right) dx \end{aligned} \tag{19}$$

$$\begin{aligned} F_i^1 &= \int_{x_a}^{x_b} q\varphi_i^{(1)} \, dx + Q_i \\ F_j^2 &= Q_j \\ Q_1 &\equiv -\hat{V}_x \;\; x_a \;\; , Q_2 \equiv -M_{xy} \;\; x_a \;\; , Q_3 \equiv -\hat{V}_x \;\; x_b \;\; , Q_4 \equiv M_{xy} \;\; x_b \\ Q_5 &\equiv -\hat{M}_{xy} \;\; x_a \;\; , Q_6 \equiv \hat{M}_{xy} \;\; x_b \end{aligned} \tag{20}$$

4 Discussion of Numerical Results

In this section we will compare the efficiency of the Finite Element Method applied to ESL (FEM-ESL) theories. For the static case, a comparison will be made between the displacement fields, transverse and longitudinal, and the stress, normal and shear fields, for laminated composite beams subjected to sine loading. Both the number of layers (one, three and four) and the stack configuration (0º, 0/90º/0 and 0/90º/90º/0, Figure 3)

The angle that the fibers form with the main axis of the beam were considered in the response field analysis. The relationship L/h considered in these examples was 4, that is, a moderately thick beam where the effects due to shear become prominent over those of flexion. In these analyzes, the results obtained by FEM-ESL are compared with the analytical ones developed by Pagano [12]. For dynamic analysis, the same beam of Figure 3 subjected to free vibration will be considered. In this example, the beam considered has the stacking configuration equal to 0º/90º/0º and relationship L/h varying in 100, 10 and 5.

The results obtained by FEM-ESL will be compared to those obtained by the three-dimensional FEM shown in Carrera [13]. In all examples we considered the graphite-epoxy material whose modulus of elasticity and Poisson's coefficients are:

$E_x = 25MPa \qquad G_{xy} = 0.5MPa$

$E_y = 1MPa \qquad G_{yz} = 0.2MPa$

$v_{xy} = v_{yz} = 0.25$

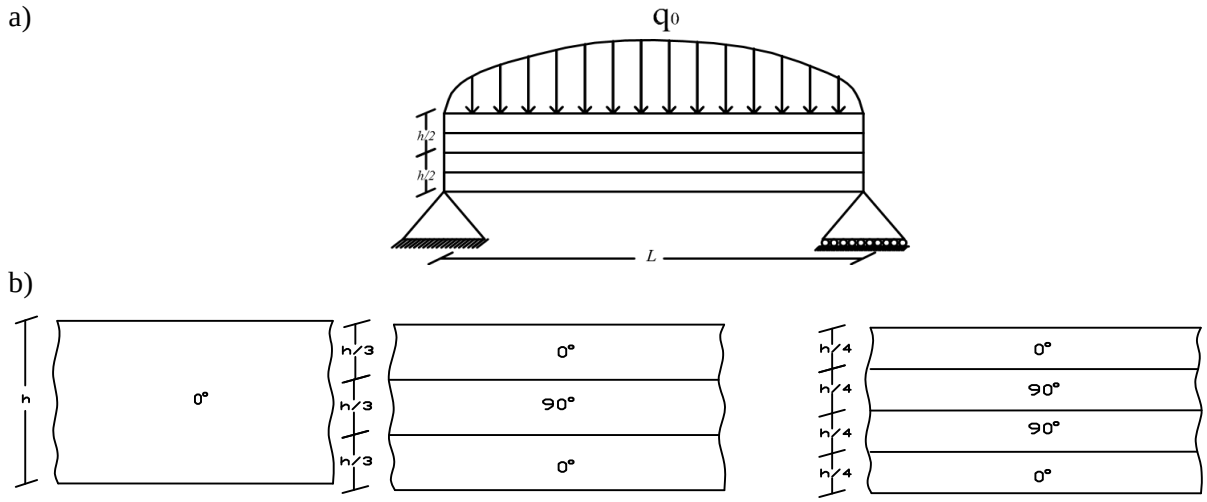

Figure 2 a) Simply supported beam subjected to a sinusoidal load, (b) arrangement of fibers in laminated beams

For the results to be independent of the geometric and loading parameters, the response fields were dimensioned as follows:

$$\begin{aligned}
&\bar{u}\left(0,z,0\right) = \frac{uE_y b}{q_0 h};\\
&\bar{w}\left(x,0\right) = \frac{100wE_y bh^3}{q_0 L^4};\\
&\bar{\sigma}_x\left(\frac{L}{2},z,0\right) = \frac{b\sigma_x}{q_0};\\
&\bar{\tau}_{xz}\left(0,z,0\right) = \frac{b\tau_{zx}}{q_0};\\
&\bar{\omega} = \omega\left(L^2\sqrt{\frac{\rho bh}{A_0}}\right) \text{ and } S = \frac{L}{h}.
\end{aligned} \qquad (21)$$

Where $\bar{u}$ is the dimensionless longitudinal displacement of the cross section, is the dimensionless deflection in the middle of the gap, $\bar{\sigma}_x$ is the dimensionless normal stress, $\bar{\tau}_{xz}$ is the dimensionless shear stress, q_0 is the amplitude of the sinusoidal loading and $\bar{\omega}$ is the natural frequency of the first vibration mode. The error calculation was given by Standard L2, with the following expression:

$$\text{relative error}_{L2}(\%) = \frac{\sqrt{(VR_1 - VC_1)^2 + (VR_2 - VC_2)^2 + ... + (VR_n - VC_n)^2}}{\sqrt{(VR_1)^2 + (VR_2)^2 + ... + (VR_n)^2}} \times 100\%. \qquad (22)$$

Where VR_i and VC_i $(i = 1, 2...n)$ are reference values and calculated respectively.

4.1 Static Analysis

4.1.1 An angled layer of the fibers at 0º

In the Figure 3(a – d), the results for the displacement and stress fields are shown when various kinematics are used in conjunction with the approximate 16-element FEM-ESL for deflection, w, by Hermite cubic polynomials and the rotation ϕ approximated by Lagrange's quadratic polynomials. In the Figures 4(a –d) the error in L_2-norm between the various kinematics used and the reference solution (Pagano[12]) is shown, as the number of elements is increased. Figure 3 shows the good agreement of the results obtained by the various FEM-ESL kinematics and the reference solution. Already in Figure 4 The convergence of the results after the use of 8 elements is evidenced. Still referring to Figure 4, It is observed that the parabolic kinematics proposed by Reddy[2], Ambartsumyam[3] and Shi-Voyiadjis[4] present the same results for the response fields analyzed. In addition to these parabolic kinematics we have to Soldatos [5] as the models with the best performance with errors below 4% in any of the response fields analyzed. In contrast, the model de Ferreira et al. [9] presented worse performances, with errors below 12%.

a)

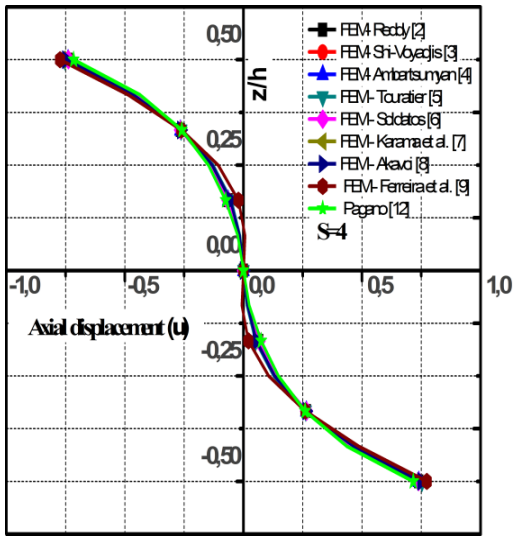

b)

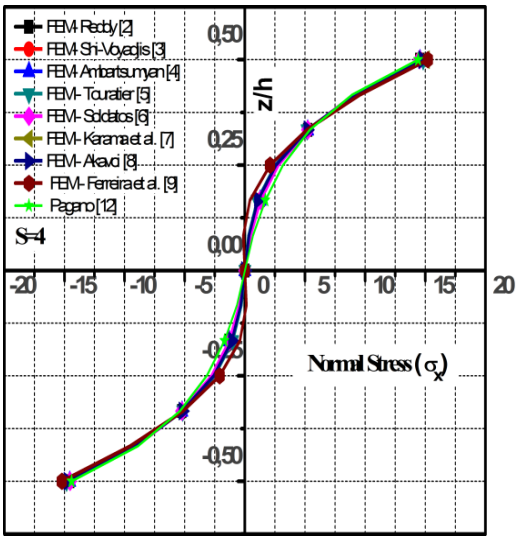

c)

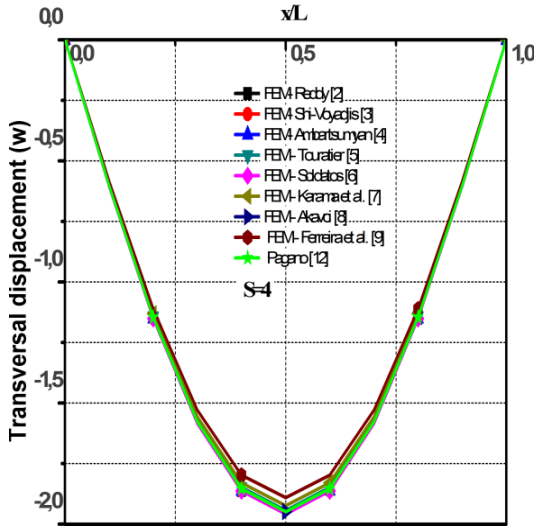

d)

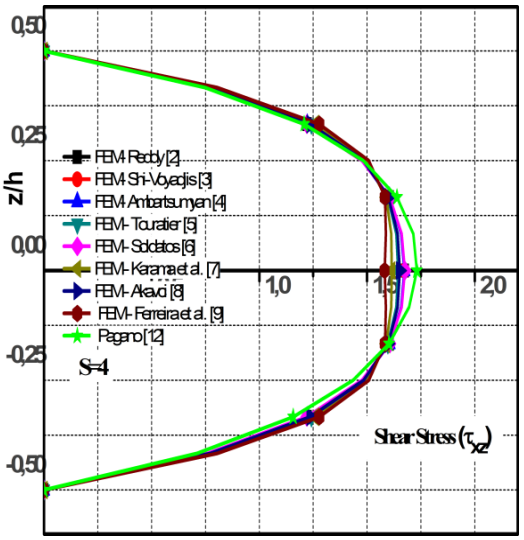

Figure 3. Field of (a) axial displacement, (b) normal stress, (c) transverse deflection along the beam, (d) shear stress when using 16-element FEM-ESL. Response fields (a) and (d) are referenced to x = L and fields (b) and (c) are referenced to x = L / 2 to the beam of (0).

a)

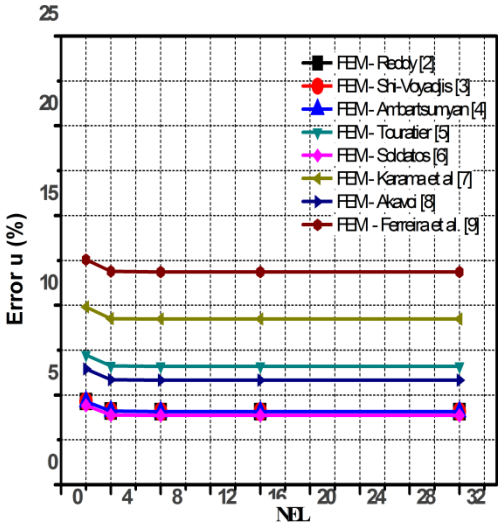

b)

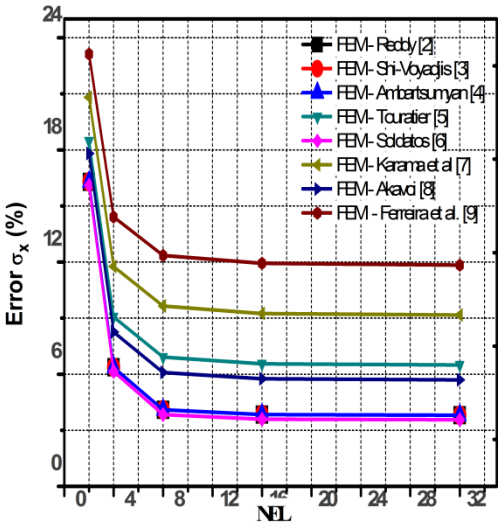

c) d)

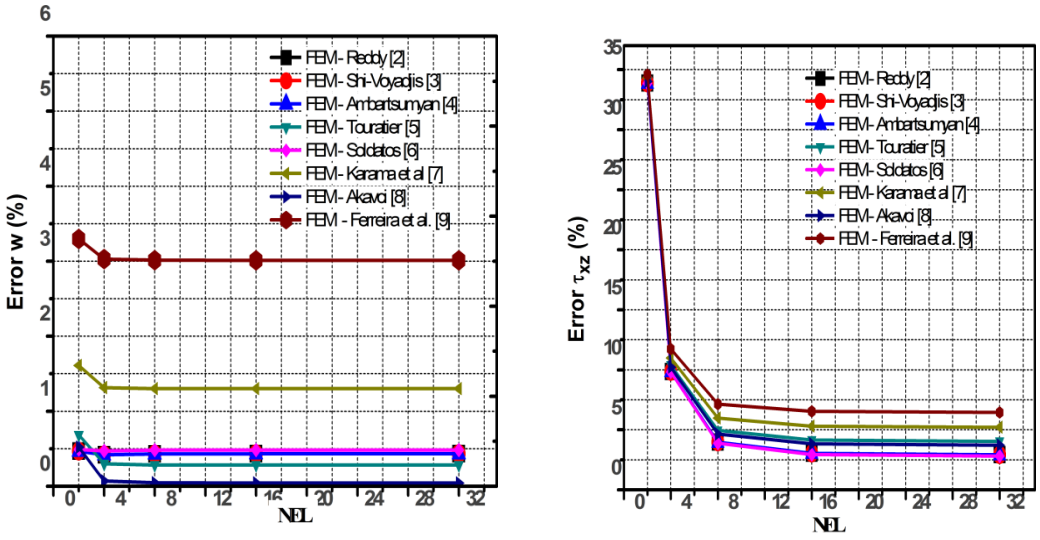

Figure 4 Standard L2 for the error of a) axial displacement, b) normal stress, c) transverse deflection and d) shear stress. as the number of elements increases (NEL Response fields (a) and (d) are referenced to x = L and fields (b) and (c) are referenced to x = L / 2 to the beam of (0º).).

4.1.2 Three layers with fiber angle at 0º / 90º / 0º

For this example, the main limitations of the ESL theory were highlighted. The approximation performed in the Figures 5(a-d) is again Hermite's cubic to w, and Lagrange's quadratic ϕ, with 16 elements. For axial displacement, although ESL theories recover the maximum value of this displacement, the kinematics coupled with the ESL theory do not exhibit the expected zigzag behavior (see Figure 6a). In relation to the tensions, the ESL theories did not recover the reference values in the interlaminar region (see Figures 6b and 6d). This is due to the use of a class C1 displacement field, thus the shear strain field is also continuous causing a discontinuous shear stress field since each layer has a different shear modulus. To overcome this obstacle, the shear stress was obtained by means of the elasticity equilibrium equations, allowing a continuity in the shear stress (see Figure 6d). Figure 7 shows the error in the L2 standard for the analyzed response fields. It is observed that the parabolic theories of Reddy[2], Shi-Voyiadjis[3] and Ambartsumyan[4] have the same error in stress and displacement (see Figure 6), and differing only in the behavior of rotation. Unlike the previous example, the models ESL de Karama et al. [8] and Ferreira et al [9] show the best results. While by the model of Ferreira et al. [9] less than 20%, 12.5%, 4% and 1% errors were obtained for the longitudinal displacement, axial stress, deflection, and shear stress fields, respectively, the parabolic and trigonometric theories had errors for the same response fields. respectively around 32%, 21%, 6% and 5%.

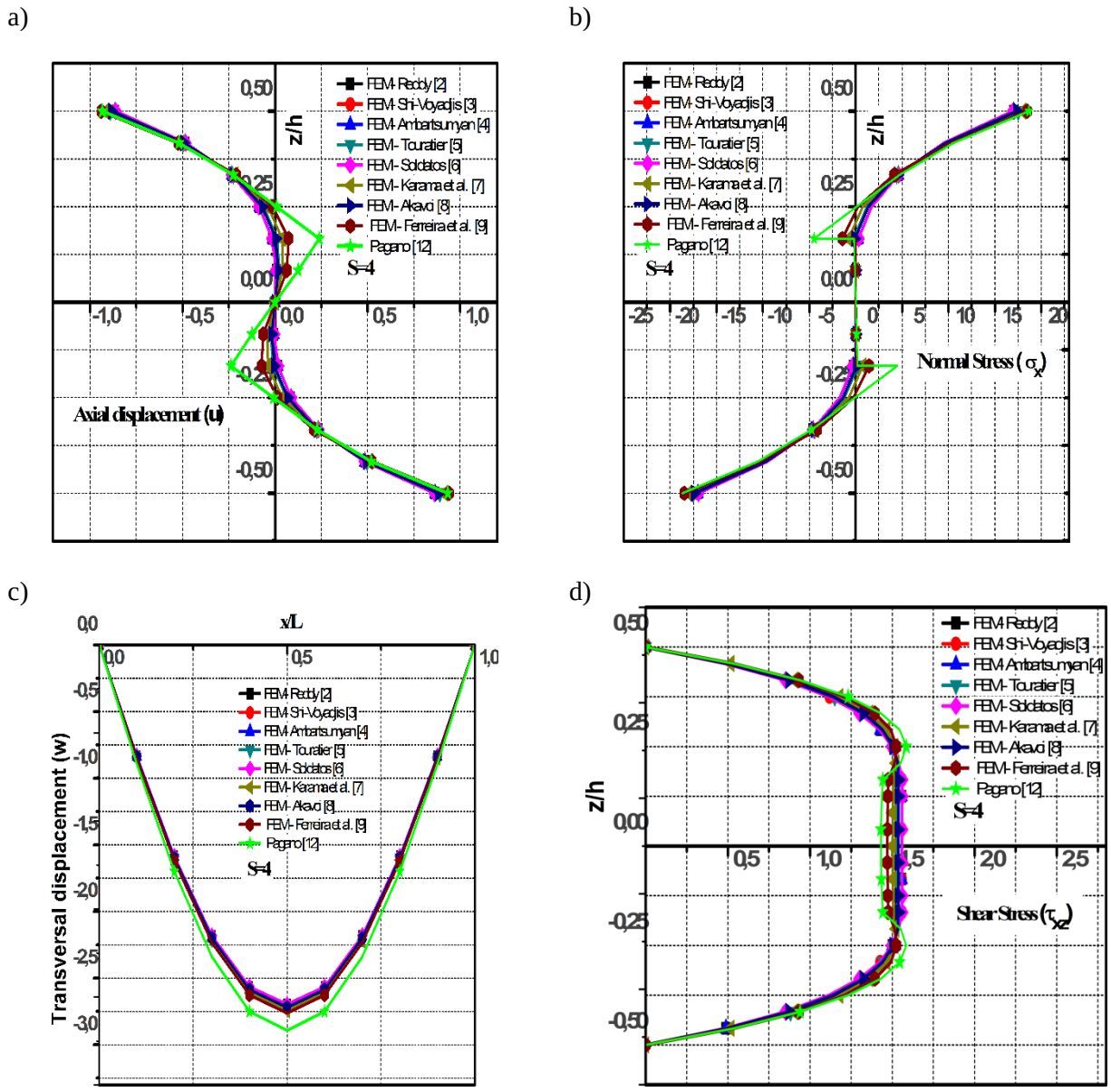

Figure 5. Behavior in the center section of the beam for (a) axial displacement, (b) normal stress, (c) transverse deflection along the beam, (d) shear stress when using 16-element FEM-ESL. Response fields (a) and (d) are referenced to x = L and fields (b) and (c) are referenced to x = L / 2 to the beam of (0º / 90º / 0º).

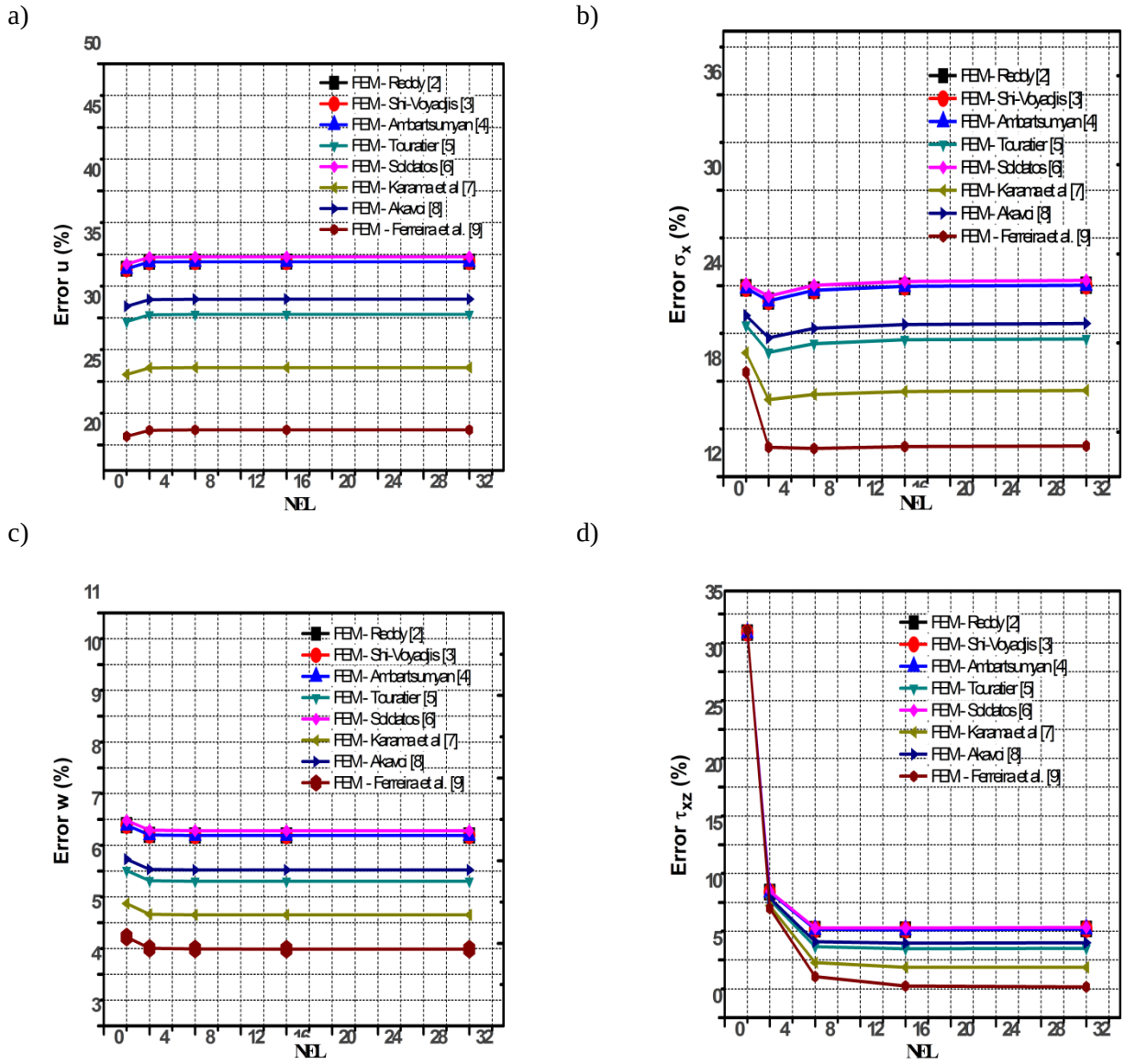

Figure 6. Standard L2 for the error of a) axial displacement, b) normal stress, c) transverse deflection and d) shear stress as the number of elements (NEL) increases. Response fields (a) and (d) are referenced to x = L and fields (b) and (c) are referenced to x = L / 2 to the beam of (0º / 90º / 0º).

4.1.3 Four layers with fiber angle at 0º / 90º / 90º / 0º

For this example was used, again 16 elements and with the same approximate polynomials of the previous example. From the results presented in the Figures 7(a-d) It is possible to observe the same limitations obtained in the previous example. However, there was an improvement in the approximation of all fields analyzed. This shows that there is a proportionality between the number of beam layers and the efficiency of the ESL theory. It should be noted again that the theory of Ferreira et al. [9] was superior to the others obtaining errors smaller than 6% (see Figure 7) for all response fields. It is observed by for all response fields. Look for all response fields. It is observed bye by Figure 8 that the error is stabilized from 8 elements.

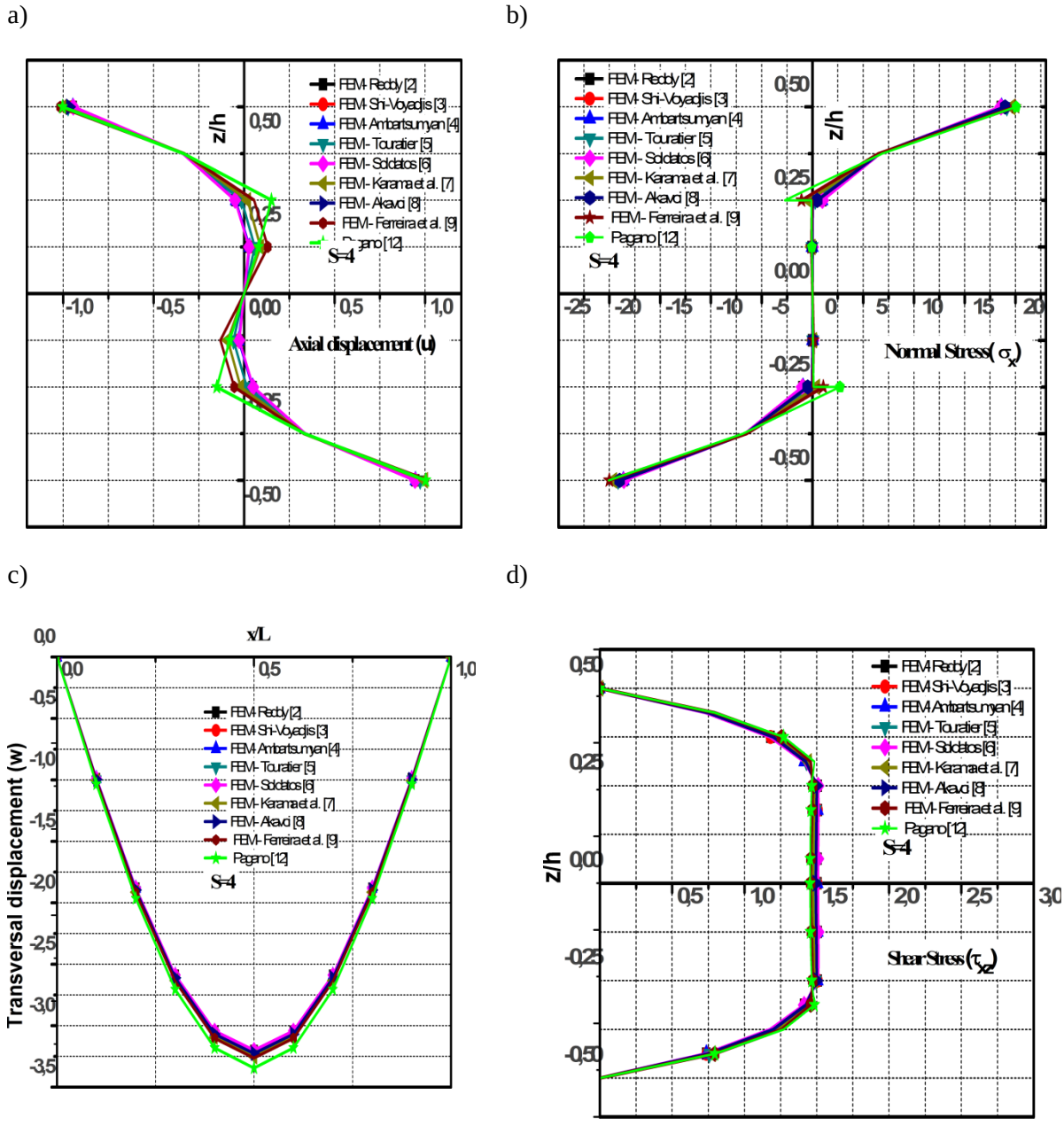

Figure 7. Field of (a) axial displacement, (b) normal stress, (c) transverse deflection along the beam, (d) shear stress when using 16-element FEM-ESL. Response fields (a) and (d) are referenced to x = L and fields (b) and (c) are referenced to x = L / 2 to the beam of (0º / 90º / 90º / 0º).

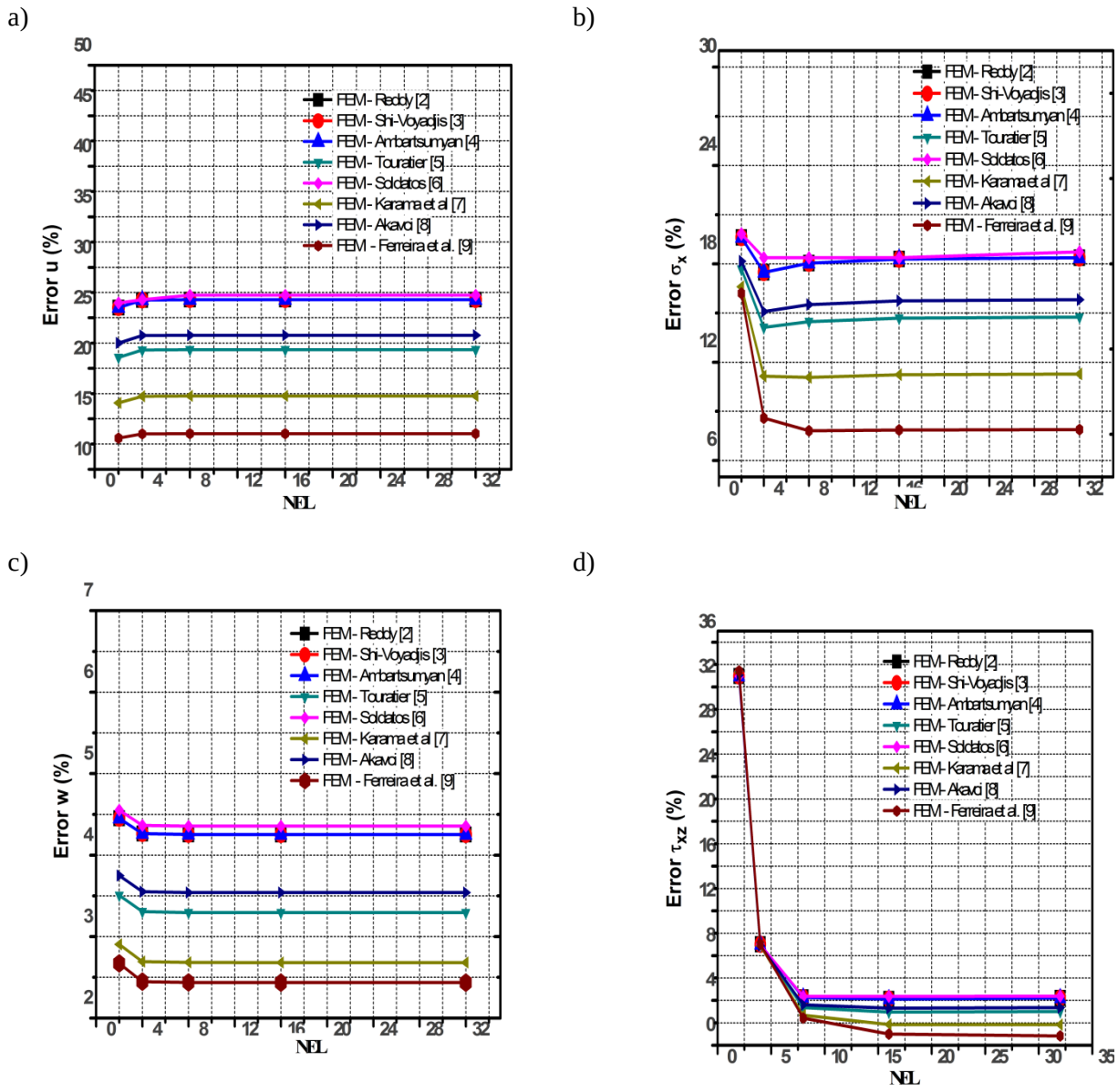

Figure 8. Standard L2 for the error of a) axial displacement, b) normal stress, c) transverse deflection and d) shear stress as the number of elements increases (NEL. S Response fields (a) and (d) are referenced to x = L and fields (b) and (c) are referenced to x = L / 2 for the beam of (0º / 90º / 90º / 0º).

4.2 Shear Locking

The shear locking effect corresponds to not recovering the correct response field as the beam becomes thin. To show the absence of this effect is shown in Figure 9 the maximum transverse displacement of a beam (0º / 90º / 0º) using FEM - ESL (16 elements), as the L / h (S) ratio increases. In addition to the theories developed here is also shown the Euler-Bernoulli (EBT) theory which has a field of response independent of the value of S. It is evident that all theories seek to recover the exact value found in Pagano [12] for both moderately thick and thin beams.

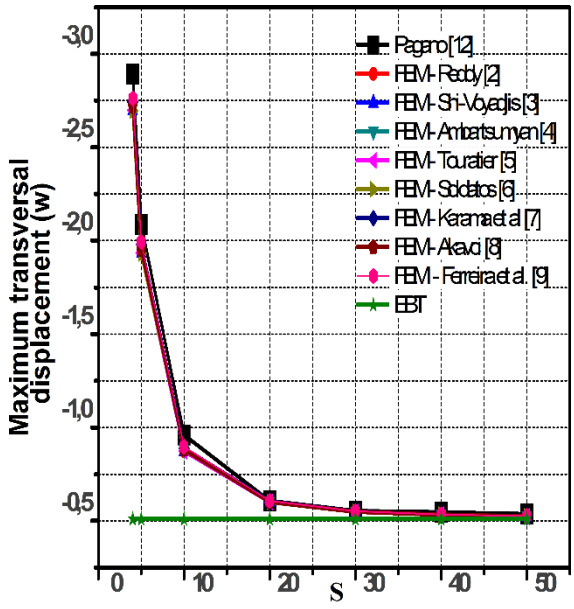

Figure 9. Maximum transverse displacement $\bar{w}$ beam (0º / 90º / 0º) as the L / h ratio increases.

4.3 Free vibration analysis

The natural frequency is obtained by solving the eigenvalue problem proposed in Eqs. (10a and 10b), via the Finite Element Method. So the approximation for vibration modes $W(x)$ and $S(x)$ is shown in Eq. (22)

$$W\ \ x\ \ \approx \sum_{i=1}^{m} W_i \varphi_i^{(1)}(x),\ \ S(x) \approx \sum_{j=1}^{n} S_j(t) \varphi_j^{(2)}(x). \tag{23}$$

where $\varphi_j^{(1)}$ and $\varphi_j^{(2)}$ they are Hermite cubic and Lagrange quadratic polynomial interpolation functions, respectively. The finite element model is given by:

$$\left(\begin{bmatrix} [K^{11}] & [K^{12}] \\ [K^{21}] & [K^{22}] \end{bmatrix} - w^2 \begin{bmatrix} [M^{11}] & [M^{12}] \\ [M^{21}] & [M^{22}] \end{bmatrix} \right) \begin{Bmatrix} \{W\} \\ \{S\} \end{Bmatrix} = \begin{Bmatrix} 0 \\ 0 \end{Bmatrix}. \tag{24}$$

To show the efficiency of the model proposed in Eq. 23 is considered a simply supported beam subject to free vibration. The stacking conFiguretion used was 0^o / 90^o / 0^o and its L / h ratio ranged from 100, 10 and 5. It was observed a convergence of the model using 8 elements, therefore, Table 2 shows a comparison between the FEM- ESL (8 elements) and the three-dimensional FEM solution shown in Giunta et al. [13]. The natural frequency obtained was dimensioned according to Eq. 21. It is evident that all theories have a good efficiency in obtaining the natural frequency $\bar{\omega}$ with relative errors less than 3.4%. Among the presented theories, Ferreira et al. It was more prominent with a maximum error of only 2% for all cases analyzed, while parabolic theories again showed no divergence in their response field. It is also worth mentioning the efficiency of FEM-ESL for both thin and moderately thick beams.

Table 2. Natural frequency $\bar{\omega}$ for a beam (0º / 90º / 0º) simply supported.

Author	S = 100	S = 10	S = 5
Reddy [2]	13,957	10,683	7,182
Shi-Voyiadjis [3]	13,957	10,683	7,182
Ambartsumyan [4]	13,957	10,683	7,182
Touratier [5]	13,956	10,636	7,142
Soldatos [6]	13,957	10,687	7,186
Karama et al. [7]	13,955	10,593	7,107
Akavci [8]	13,956	10,649	7,152
Ferreira et al. [9]	13,953	10,546	7,071
FEM 3D [13]	13,932	10,334	6,888

5 Conclusions

In the present work a finite element model was developed for several high order ESL theories. To highlight the efficiency of the model, examples were made for both static bending and free vibration analysis. It was found that for a single layer the parabolic and trigonometric theories [2-6] obtain excellent results, while for a larger number of layers the theories of Ferreira et al. [9] and de Karama et al. [7] are superior. This has been proven in both static and dynamic analysis. Overall, ESL theories yield good results for global response fields such as transverse displacement and natural beam frequency. However, for local domains such as in the interlaminary regions, ESL theories are not efficient because they do not describe the zigzag behavior of in-plane displacement. Finally, regarding FEM-ESL, with the use of 8 elements it is possible to obtain excellent results for all the theories described here.

Acknowledgements

The authors would like to acknowledge Federal University of Sergipe (PIBIC/COPES), Coordenação de Aperfeiçoamento de Pessoal de Nível Superior – Brazil (CAPES) – Finance code 001 for the financial. support

References

[1] Timoshenko S.P.. *On the correction for shear of the differential equation for transverse vibrations of prismatic bars*, fiilosophical Magazine 41, 744-746, 1921

[2] J.N. Reddy. *A simple higher-order theory for laminated composite plates. Journal of Applied Mechanics*, v. 51, n. 4, p. 745–752, 1984.

[3] G. Shi and G.Z. Voyiadjis. *A Sixth-Order Theory of Shear Deformable Beams With Variational Consistent Boundary Conditions*. Journal of Applied Mechanics, v. 78, n. 2, p. 21019, 2011.

[4] S.A. Ambartsumyan. *On theory of bending plates*. Izv Otd Tech Nauk AN SSSR, v. 5, n. 5, p. 69–77, 1958.

[5] M. Touratier, *An efficient standard plate theory*, Int. J. Eng. Sci., vol. 29, no. 8, pp. 901–916, 1991.

[6] K.P. Soldatos, *A transverse shear deformation theory for homogeneous monoclinic plates*, Acta Mechanica, vol. 94, pp. 195–200, 1992.

[7] M. Karama , K. S. Afaq and S. Mistou, *Mechanical behavior of laminated composite beam by new multi-layered laminated composite structures model with transverse shear stress continuity*, Int. J. Solids Struct.,, pp. 1525–1546, 2003.

[8] S. S. Akavci, *Buckling and free vibration analysis of symmetric and anti-symmetric laminated composite plates on an elastic foundation*, J. Reinf. Plast. Compos., vol. 26, no. 18, pp. 1907–1919, 2007.

[6] K.P. Soldatos, *A transverse shear deformation theory for homogeneous monoclinic plates*, Acta Mechanica, vol. 94, pp. 195–200, 1992.
[7] M. Karama , K. S. Afaq and S. Mistou, *Mechanical behavior of laminated composite beam by new multi-layered laminated composite structures model with transverse shear stress continuity*, Int. J. Solids Struct.,, pp. 1525–1546, 2003.
[8] S. S. Akavci, *Buckling and free vibration analysis of symmetric and anti-symmetric laminated composite plates on an elastic foundation*, J. Reinf. Plast. Compos., vol. 26, no. 18, pp. 1907–1919, 2007.
[9] A. J. Ferreira, Thai, C.H.,S.P. Bordas,T. Rabczuk and H. Nguyen-Xuan . *Isogeometric analysis of laminated composite and sandwich plates using a new inverse trigonometric shear deformation theory. Eur J Mech* – A Solids;43:89–108, 2014.
[10] S. A. Sayyad and Y. M. Ghugal . *Flexural analysis of fibrous composite beams under various mechanical loadings using refined shear deformation theories.* Composites: Mechanics, Computations, Applications. An International Journal 5(1), 1–19, 2014.
[11]J. N. Reddy. *Mechanics of laminated composite plates and shells. Theory and analysis*. Boca Raton: CRC Press; 2004.
[12] N. J. Pagano. *Exact solution for composite laminates in cylindrical bending*. J Compos Mater 1969;3:398–411.
[13] G. Giunta ,F. Biscani, S. Belouettar, et al. *Free vibration analysis of composite beams via refined theories*. Compos: Part B; 44: 540–552, 2013.
[14] J. N. Reddy. *Energy and Variational Methods in Applied Mechanics*.. New York: John Wiley, 1984.